

# Dependence of pathogen molecule-induced Toll-like receptor activation and cell function on Neu1 sialidase

Schammim Ray Amith · Preethi Jayanth · Susan Franchuk · Sarah Siddiqui · Volkan Seyrantepe · Katrina Gee · Sameh Basta · Rudi Beyaert · Alexey V. Pshezhetsky · Myron R. Szewczuk

Received: 6 November 2008 / Revised: 19 February 2009 / Accepted: 6 April 2009 / Published online: 9 May 2009  
© Springer Science + Business Media, LLC 2009

**Abstract** The signaling pathways of mammalian Toll-like receptors (TLR) are well characterized, but the initial molecular mechanisms activated following ligand interactions with the receptors remain poorly defined. Here, we show a membrane controlling mechanism that is initiated by ligand binding to TLR-2, -3 and -4 to induce Neu1 sialidase activity within minutes in live primary bone marrow (BM) macrophage cells and macrophage and dendritic cell lines. Central to this process is that Neu1 and not Neu2, -3 and -4 forms a complex with TLR-2, -3 and -4 on the cell surface of naïve macrophage cells. Neuraminidase inhibitors BCX1827, 2-deoxy-2,3-dehydro-*N*-acetylneuraminic acid (DANA), zanamivir and oseltamivir carboxylate have a limited significant inhibition of the LPS-induced sialidase activity in live BMC-2 macrophage cells but Tamiflu (oseltamivir phosphate) completely blocks this activity. Tamiflu inhibits LPS-induced sialidase activity

in live BMC-2 cells with an  $IC_{50}$  of 1.2  $\mu$ M compared to an  $IC_{50}$  of 1015  $\mu$ M for its hydrolytic metabolite oseltamivir carboxylate. Tamiflu blockage of LPS-induced Neu1 sialidase activity is not affected in BMC-2 cells pretreated with anticomplexing agent clopidogrel. Endotoxin LPS binding to TLR4 induces Neu1 with subsequent activation of NF $\kappa$ B and the production of nitric oxide and pro-inflammatory IL-6 and TNF $\alpha$  cytokines in primary and macrophage cell lines. Hypomorphic cathepsin A mice with a secondary Neu1 deficiency respond poorly to LPS-induced pro-inflammatory cytokines compared to the wild-type or hypomorphic cathepsin A with normal Neu1 mice. Our findings establish an unprecedented mechanism for pathogen molecule-induced TLR activation and cell function, which is critically dependent on Neu1 sialidase activity associated with TLR ligand treated live primary macrophage cells and macrophage and dendritic cell lines.

S. Amith · P. Jayanth · S. Franchuk · S. Siddiqui · K. Gee · S. Basta · M. R. Szewczuk (✉)  
Department of Microbiology & Immunology, Queen's University, Kingston, ON K7L3N6, Canada  
e-mail: szewczuk@queensu.ca

V. Seyrantepe · A. V. Pshezhetsky  
Departments of Pediatrics and Biochemistry, Montreal University, Service de Genetique, Ste-Justine Hospital, 3175 Cote-Ste-Catherine, H3T1C5 Montreal, QC, Canada

R. Beyaert  
Department for Molecular Biomedical Research, VIB, Unit for Molecular Signal Transduction in Inflammation, Technologiepark 927, B-9052 Zwijnaarde, Belgium

R. Beyaert  
Department of Biomedical Molecular Biology, Ghent University, Ghent, Belgium

**Keywords** Toll-like receptors · Neu1 sialidase · NF $\kappa$ B activation · pro-inflammatory cytokines · Neu1 deficient mice

## Abbreviations

(TLR)	Toll-like receptors
(PAMPS)	pathogen-associated molecular patterns
(oseltamivir phosphate)	Tamiflu
(DANA)	2-deoxy-2,3-dehydro- <i>N</i> -acetylneuraminic acid
(IL-6)	interleukin-6
(TNF $\alpha$ )	tumor necrosis factor
(LPS)	lipopolysaccharide
( $IC_{50}$ )	50% inhibition concentration
(ECD)	ectodomain
(poly:IC)	polyinosinic-polycytidylic acid

(TS)	<i>T. cruzi</i> trans-sialidase
(BM)	bone marrow
(M-CSF)	monocyte colony-stimulating factor
(4-MUNANA (4-MU))	[2'-(4-methylumbelliferyl)- $\alpha$ - <i>N</i> -acetylneuraminic acid]
(PVDF)	polyvinylidene fluoride
(NO)	nitric oxide
(Neu1-CathA KD)	hypomorphic cathepsin A mice with the secondary ~90% reduction of the Neu1 activity
(CathA KI)	normal Neu1 sialidase bound to inactive cathepsin A Ser190Ala mutant
(Neu4 KO)	Neu4 knockout

## Introduction

Mammalian Toll-like receptors (TLRs) are a family of receptors that recognize pathogen-associated molecular patterns (PAMPS). They play key roles in activating immune responses during infection by linking the host's innate and adaptive immune responses against pathogen infections. Studies of the crystal structure at 2.1 angstroms of human TLR3 ectodomain (ECD) reveal a large horseshoe-shaped solenoid which is highly glycosylated with several *N*-linked glycosylation sites contributing significantly to the additional mass of TLR3 ECD [1]. Structural studies of TLR ECD have also revealed a single sterically unhindered sugar-free face [1–5], which may be involved in the formation of the dimerization interface. Glycosylation has been shown to be a common property of a number of TLRs, including TLR-2,-3, and-4 [4, 6, 7]. Lack of glycosylation or mutation of glycosylated residues has been shown to negatively affect not only the receptor's ability to transduce signals, but also maintenance of receptor complexes [4, 6, 7]. Taken together, these findings suggest that glycosylation of TLRs may play a critical role in receptor activation and its modification may be a cellular mechanism of controlling TLR activation in promoting dimerization. To date, the precise role of *N*-linked glycosylation in TLR receptor activation and cell function following their pathogen-molecule interactions has not been defined.

Insight for the role of glycosylation in TLR activation came from the well-characterized model of TrkA tyrosine-protein kinase receptor family, which functions as signaling receptors for the neurotrophin family of molecules of nerve growth factor (NGF). For NGF TrkA receptors, glycosylation of the receptor is required to localize the receptors to the cell surface, where it prevents ligand-independent activation of receptors [8]. Recently, we discovered a membrane sialidase-controlling mechanism that depends on neuro-

trophin growth factors binding to their specific TrkA and TrkB receptors to induce sialidase activity [9, 10]. The sialidase targets and desialylates Trk and, consequently causes the induction of receptor dimerization and activation. We also identified a specific sialyl  $\alpha$ 2-3-linked  $\beta$ -galactosyl sugar residue of TrkA, which was rapidly targeted and hydrolyzed by the activated sialidase [9].

Here, we report that Neu1 sialidase and not Neu2,-3 and-4 forms a complex with TLR-2,-3 and-4 receptors. Neu1 is expressed on the cell surface membrane of primary macrophage cells and macrophage cell lines. Activation of Neu1 is induced by TLR ligands binding to their respective receptors. The neuraminidase inhibitor Tamiflu (oseltamivir phosphate) completely inhibits Neu1 sialidase activity associated with the TLR ligand treated live macrophage cells. Also, Tamiflu significantly inhibits endotoxin LPS induced NF $\kappa$ B activation and the production of nitric oxide and pro-inflammatory IL-6 and TNF $\alpha$  cytokines in primary or macrophage cell lines. Primary macrophages obtained from hypomorphic cathepsin A mice with a secondary Neu1 deficiency respond poorly to LPS-induced pro-inflammatory cytokines. These findings reveal an unprecedented mechanism of pathogen-molecule induced TLR activation and cell function. Neu1 sialidase may be a key regulator of TLR activation to generate a functional receptor.

## Materials and methods

**Reagents** TLR4 ligand lipopolysaccharide (LPS, 1fg/mL to 3  $\mu$ g/mL, from *Serratia marcescens* and purified by phenol extraction; Sigma, St. Louis, MO), TLR2 ligand Zymosan A (200  $\mu$ g/ml, from *Saccharomyces cerevisiae*; Sigma, St. Louis, MO) TLR3 ligand polyinosinic-polycytidylic acid (poly I:C, 20  $\mu$ g/ml; Sigma) were used at the indicated optimal dosage. TLR2 ligands, killed *Mycobacterium butyricum* (5  $\mu$ g/ml, DIFCO) and killed highly virulent human Brazil strain *Trypanosoma cruzi* parasites ( $2 \times 10^6$  parasites/ml) (kind gift from Dr Cheryl Davis, Western Kentucky University, Bowling Green, Ky, USA) were used at indicated optimal dosage.

The sialidase substrate, 2'-(4-methylumbelliferyl)- $\alpha$ -*N*-acetylneuraminic acid (98% pure, 4-MUNANA or 4-MU, Biosynth International Inc., Itasca, IL, USA) was used at optimal concentration of 0.318 mM for the live cell sialidase assay.

Tamiflu (99% pure oseltamivir phosphate, Hoffmann-La Roche Ltd., Mississauga, Ontario, Lot # BS00060168) was used at indicated concentrations as well as highly purified compounds of BCX-1812 and BCX-1827 (BioCryst Pharmaceuticals Inc., Birmingham, AL), and DANA (2-deoxy-2,3-dehydro-*N*-acetylneuraminic acid, Sigma). Pure compounds

of zanamivir, oseltamivir phosphate and oseltamivir carboxylate were kindly provided by Prof. Mark von Itzstein, Griffith University Institute for Glycomics, Queensland). Clopidogrel bisulfate (Plavix, Bristol-Myers Squibb), an antiplatelet and anticarboxylesterase agent was used at indicated concentrations. The optimal dose of 200 ng of recombinant *T. cruzi* trans-sialidase (TS) per ml was used as predetermined elsewhere [11].

**Cell lines** BMC-2 and BMA macrophage cells [12] and DC2.4 dendritic cells [13] were obtained from Dr Ken L. Rock, University of Massachusetts Medical School, Worcester, MA. The HEK293 parental cell line was a gift from Dr Leda Raptis of the Department of Microbiology & Immunology, Queen's University, Kingston, Ontario. THP-1 cells (American Type Culture Collection [ATCC]) were grown in 1x IMDM (Iscove's Modified Dulbecco's Medium, HyClone, Fisher Scientific Co., Ottawa, Ontario) supplemented with 5% fetal calf serum (FCS). Stable HEK-TLR cells were obtained by calcium phosphate transfection of a pCDNA3 expression vector for a specific chimeric TLR with an in frame C-terminal YFP and selection in 0.4 µg/ml G418. The HEK-TLR4/MD2 cell line was generated by additional co-transfection of an expression plasmid for human MD2. All cells were grown at 37°C in 5% CO<sub>2</sub> in culture media containing DMEM (Gibco, Rockville, MD) supplemented with 5% horse serum (Gibco) and 3% fetal calf serum (FBS) (HyClone, Logan, Utah, USA).

**Primary mouse bone marrow macrophage cells** Bone marrow (BM) cells were flushed from femurs and tibias of mice with sterile Tris-buffered saline (TBS) solution. The cell suspension was centrifuged for 3 min at 900 rpm, and the cell pellet resuspended in red cell lysis buffer for 5 min. The remaining cells were washed once with sterile TBS, and then resuspended in RPMI conditioned medium supplemented with 10% FBS and 20% (v/v) of L929 cell supernatant as a source of monocyte colony-stimulating factor (M-CSF) according to Alatery and Basta [14] and 1x L-glutamine-penicillin-streptomycin (Sigma-Aldrich Canada Ltd., Oakville, Ontario) sterile solution. The primary BM macrophages were grown on 12mm circular glass slides in RPMI conditioned medium for 7–8 days in a humidified incubator at 37°C and 5% CO<sub>2</sub>. Primary BM macrophage cells by day 7 are more than 95% positive for macrophage marker F4/80 molecule as detected by flow cytometry.

**Sialidase activity in viable cells** Primary bone marrow macrophages and TLR-expressing cells were grown on 12 mm circular glass slides in conditioned medium as described above. After removing medium, 0.318 mM 4-MUNANA (4-MU) substrate [2'-(4-methylumbelliferyl)-α-

*N*-acetylneuraminic acid] (Biosynth International Inc., Itasca, IL, USA) in Tris buffered saline pH7.4 was added to each well alone (control), with predetermined dose of TLR specific ligand (LPS, 3–5 µg/mL; Zymosan A, 200 µg/mL from *Saccharomyces cerevisia*; polyinosinic-polycytidylic acid (poly I:C), 20 µg/ml), or in combination of TLR ligand and 200–500 µM Tamiflu as previously described [9]. The substrate is hydrolyzed by sialidase to give free 4-methylumbelliferone, which has a fluorescence emission at 450 nm (blue color) following an excitation at 365 nm. Fluorescent images were taken after 1–2 min using epi-fluorescent microscopy (40x objective).

**Fluorescence spectrophotometer analysis of LPS-induced sialidase activity in cell suspensions of BMC-2 macrophage cells** Cells at 90% confluence in 25-cm<sup>2</sup> flasks were resuspended in 500 mL of serum-free Tris-buffered medium pH7.4. To 50 mL of cell suspension (0.3 to 1.26x10<sup>6</sup> cells/mL) in black 96-well fluorescence plates was added 0.318mM 4-MUNANA with or without the presence of 3 µg/ml LPS. The fluorescence intensity readings were immediately taken over 30 min using the Varioskan Fluorescence Spectrophotometer (Type 3001, Microplate Instrumentation, Thermo Electron Corporation, Vantaa, Finland) at emission 450 nm following an excitation at 365 nm. The sialidase activity in the cell samples corrected for background endogenous sialidase activity in untreated cells was calculated from a standard neuraminidase activity curve, and expressed as milli Units per mg of 4-MUNANA (4-MU) for the indicated cell concentrations.

**Immunocytochemistry of NFκB** Primary BM macrophages and TLR-expressing cells were pretreated with pure Tamiflu at indicated concentrations for 1 h followed with predetermined dose of TLR specific ligands for 45 min. Cells were fixed with 4% paraformaldehyde, permeabilized with Triton-X100 and immunostained with rabbit anti-NFκBp65 (Rockland, Gibertsville, PA), or rabbit anti-IκBα (Rockland) antibodies followed with Alexa Fluor594 goat anti-rabbit IgG. Stained cells were visualized by epi-fluorescence microscopy using a 40x objective. Quantitative analysis was done by assessing the density of cultured cell staining corrected for background in each panel using Corel Photo Paint 8.0 software. Each bar in the figures represents the mean corrected density of staining ± SEM for cultured cells (n) within the respective images. The cultures in each panel are of equal cell density. *P* values represent significant differences at 95% confidence using Dunnett's Multiple Comparison Test compared to control (Ctrl) in each group.

**Flow cytometry of cell surface Neu1 in live BMC-2 cells** Cells were grown in 25-cm<sup>2</sup> flasks at 90% confluence.

For cell surface staining, live cells in serum free cold phosphate-buffered saline (PBS) were stained with rabbit anti-Neu1 antibody (H-300, Santa Cruz Biotechnology, Inc. California, US) for 15–20 min at 4°C, washed and followed with Alexa Fluor488 goat anti-rabbit IgG. After washing with cold PBS buffer, the cells were prepared for flow cytometry analysis. 40000 cells were acquired on a Beckman Coulter (Miami, FL) Epics XL-MCL flow cytometer and analyzed with Expo32 ADC software (Beckman Coulter). For overlay histograms, control cells treated with Alexa488 conjugated goat anti-rabbit IgG alone are represented by the gray-filled histogram. Cells treated with anti-Neu1 antibody together with Alexa488 secondary antibody are depicted by the unfilled histogram with the black line. The mean fluorescence for each histogram is indicated for 80% gated cells.

*Flow cytometry of LPS-induced production IL-6 and TNF $\alpha$*  Monocytic THP-1 cells grown in 25-cm<sup>2</sup> flasks at 90% confluence were treated with 3  $\mu$ g/ml LPS for 16 or 48 h in the presence or absence of 200 and 400  $\mu$ M Tamiflu. They were fixed and immunostained with fluorescein conjugated anti-IL-6 antibody (16 h) or anti-TNF $\alpha$  antibody (48 h). 10,000 cells were acquired on a Beckman Coulter (Miami, FL) Epics XL-MCL flow cytometer and analyzed with Expo32 ADC software (Beckman Coulter). For overlay histograms, untreated control cells are represented by the gray-filled histogram. Cells treated with LPS are depicted by the black line. Cells treated LPS and Tamiflu are depicted by the gray-solid line (200  $\mu$ M Tamiflu) or gray-dashed line (400  $\mu$ M Tamiflu). The mean fluorescence for each histogram is indicated for 70% gated cells.

*Neu1 Colocalization with TLR* Primary BM macrophages obtained from normal, wild-type (WT) mice were cultured in RPMI medium supplemented with 20% M-CSF, 10% FCS and Penn/Strep/Glut for 8 days on circular glass slides in 24 well tissue culture plates as described above. BMC-2 cells or primary BM macrophage cells were stimulated with 5  $\mu$ g/ml LPS for 10 min or left untreated as no ligand controls. Cells were fixed, permeabilized or non-permeabilized, and immunostained with rat anti-TLR4/MD2 (MTS510, Santa Cruz Biotech) and rabbit anti-Neu1 (H-300, Santa Cruz Biotechnology, Inc., California, USA) followed with Alexa Fluor594 goat anti-rabbit IgG or Alexa Fluor488 rabbit anti-rat IgG. Stained cells were visualized using a confocal inverted microscope (Leica TCS SP2 MP inverted Confocal Microscope) with a 40x or 100x (oil) objectives. Images were captured using a z-stage of 8–10 images per cell at 0.5-mm steps.

*Western blots and co-immunoprecipitation* HEK-TLR4/MD2 cells are left cultured in media or in media containing

5  $\mu$ g/ml LPS for 5 min. Cells are pelleted and lysed in lysis buffer (50 mM Tris, pH8, 150 mM NaCl, 1% NP-40, 0.2 mg/ml leupeptin, 1%  $\beta$ -mercaptoethanol, and 1 mM phenylmethanesulfonyl fluoride (PMSF)). Cell lysates are immunoprecipitated with 2  $\mu$ g of rat anti-TLR4/MD2 (MTS510, Santa Cruz Biotechnology Inc., CA, USA) antibodies for 18 h. Following immunoprecipitation, complexes are isolated using protein G magnetic beads, washed 3x in buffer (10 mM Tris, pH8, 1 mM EDTA, 1 mM EGTA, 150 mM NaCl, 1% Triton X-100 and 0.2 mM sodium orthovanadate) and resolved by 8% gel electrophoresis (SDS-PAGE). Proteins are transferred to polyvinylidene fluoride (PVDF) transfer membrane blot. The blot is probed for either Neu1 (45.5 kDa) with anti-Neu1 (Abcam), Neu2 (42 kDa) with anti-Neu2 (Santa Cruz Biotechnology Inc.), Neu3 (48 kDa) with anti-Neu3 (MBL Medical and Biological Laboratories Co., Ltd. Japan), Neu4 (53 kDa) with anti-Neu4 (Protein Tech Group, Inc., Chicago, USA), or TLR-2,-3 and-4 with respective anti-TLR antibodies followed by HRP conjugated secondary IgG antibodies and Western Lightning Chemiluminescence Reagent Plus. The initial IP blot is stripped and further probed for described proteins. The chemiluminescence reaction is analyzed with either a Fluorochem HD2 Imaging System (Alpha Immunosci, San Leandro, CA, USA) or x-ray film. Sample concentration for gel loading was determined by Bradford reagent.

*Nitric oxide assay* Nitric oxide (NO) production was measured using Griess reagent as described previously [15]. DC2.4 dendritic cells (200  $\mu$ l/well) were cultured in phenol-red free RPMI media (Invitrogen, Ontario) containing 5% FCS (Hyclone Canadian) at 50,000 cells/well in 96-well round-bottom culture plates (Corning Inc., Corning, NY, USA). The samples were placed in a 5% CO<sub>2</sub> humidified incubator at 37°C for 18 h. All the reagents for the NO assay were purchased from Sigma-Aldrich (Oakville, Ontario). Cell-free culture supernatants (100  $\mu$ l/well) were placed in a 96-well NUNC flat bottomed MicroWell plate (Corning Inc.) and sulphanilamide solution (50  $\mu$ l) [1% w/v sulphanilamide in 5% w/v phosphoric acid] was added to each well. The plate was incubated in the dark for 10 min at room temperature, after which NED solution (50  $\mu$ l) [0.1% w/v N-1-naphthylethylenediamine dihydrochloride in water] was added followed by another 10 min incubation. Absorbance of the samples was measured at 540 nm using a Varioskan spectrophotometric microplate reader (Thermo Electron Corp., Finland). Sodium nitrite (0–100  $\mu$ M) (Fisher Scientific, Whitby, ON) dissolved in phenol-red free RPMI was used to generate a standard concentration curve.

*Cytokine array profiling and ELISA* Mice were bled before (no LPS) and 5 h after i.p. injection with 2.5 mg of LPS per

mouse. Serum was extracted and immediately analyzed for cytokine array profiling with R&D System Cytokine Array Profiling ARY066 kit (R&D Systems, Inc., Minneapolis) according to kit protocol. The chemiluminescence reaction is analyzed with either a Fluorochem HD2 Imaging System (Alpha Immunity, San Leandro, CA, USA) or x-ray film. For x-ray film, quantitative analysis was done by assessing the density of staining corrected for background in each spot using Corel Photo Paint 8.0 software. The serum was further analyzed for IL-6 cytokine using the mouse IL-6 ELISA Ready-set-go kit (eBioscience Inc., San Diego, CA) according to kit protocol.

**Statistics** Comparisons between two groups were made by one-way ANOVA at 95% confidence using unpaired t-test and Bonferroni's Multiple Comparison Test or Dunnett's Multiple Comparison Test for comparisons among more than two groups.

## Results

Sialidase activity associated with TLR ligand treated live primary bone marrow macrophage cells, and macrophage and dendritic cell lines

To determine whether or not TLR ligands induce cellular sialidase in live macrophage cells, we used a recently developed assay to detect sialidase activity on the surface of viable cells [9]. Here, we show that TLR ligands zymosan A (TLR-2), poly I:C (TLR-3) and LPS (TLR-4) induced sialidase activity on the cell surface of live BMC-2 macrophage [12] and DC2.4 dendritic [13] cells in culture after 2 min. This activity was revealed by a fluorescence ( $\lambda_{em}$  450 nm) surrounding the cells treated with the fluorogenic sialidase substrate, 4MU-NeuAc (2'-(4-methylumbelliferyl)- $\alpha$ -*N*-acetylneuraminic acid) and caused by the emission of 4-methylumbelliferone (Fig. 1a). When primary mouse BM derived macrophages were treated with the same TLR ligands, we obtained similar results to those found for the cell lines (Fig. 1a). However, TLR3 ligand polyI:C did not induce sialidase activity in these primary macrophages in contrast to what was seen in BMC-2 and DC2.4 cells. These latter data supported previous findings that transformed macrophages and dendritic cells may express TLR3 on the membrane, while this receptor is absent from the membrane in primary mouse macrophage cells [16]. If TLR receptors are involved in the process of activating sialidase(s), we should not expect to see this activity in ligand-treated TLR-deficient HEK-293 cells compared to HEK cells stably transfected with TLR2, TLR3 or TLR4/MD2. The

data showed this to be the case (Fig. 1b). Only TLR ligands specific for their receptors induced sialidase activity.

In Fig. 1, the sialidase activity as revealed by a fluorescence ( $\lambda_{em}$  450 nm) surrounding the cells was variable from being largely cell associated for TLR3 ligand poly-I:C treated BMC-2 cells to nearly totally diffused for BMC-2 cells treated with zymosan A. These observations could indicate that the relative density of TLR expression on the cell surface might be associated with sialidase inducing its activity. Furthermore, the sialidase activity induced by TLR4 ligand LPS in live BMC-2 cells was dose dependent and detectable at 1 fg/mL of LPS (Fig. 2a). Because of the diffuse fluorescence associated with TLR ligand treated cells, we questioned whether or not this fluorescence was due to a secreted sialidase(s). Medium was taken from the reaction wells containing the live cells and added immediately to 4-MUNANA substrate. A positive control sialidase (*Clostridium perfringens*), which has a specific activity of 1 U per 1 mmol of *N*-acetylneuraminic acid per minute was also added separately to the 4-MUNANA substrate. As shown in Fig. 2b, the fluorescence associated with TLR ligand treated cells as seen in Figs. 1 and 2a was not due to a form of secreted or shed sialidase from the cells. These results are consistent with our previous report on NGF-treated TrkA-expressing cells [9]. In addition, it is noteworthy that live cells treated with the substrate alone did not show any fluorescence surrounding the cells. Instead, they revealed an internal blue fluorescence indicating substrate internalization by the cell revealing internal sialidase activity (Fig. 2c). Taken together, these results suggest that the diffuse fluorescent associated with TLR ligand treated cells is due to an activation of a cellular sialidase on the cell surface.

We also tested whether this TLR ligand-induced sialidase activity could be observed in the cell suspensions of BMC-2 cells. To 50  $\mu$ L of cell suspension ( $0.3$  to  $1.26 \times 10^6$  cells/mL) from 95% cell confluence in 25-cm<sup>2</sup> flasks of serum-free medium, 3  $\mu$ g/mL LPS and 0.318 mM 4-MUNANA were added in fluorescent microtiter plates at different time intervals or were left untreated as controls. The fluorescence intensity readings were immediately taken over 30 min using the Varioskan fluorescence spectrophotometer using fluorescence emission at 450 nm and an excitation at 365 nm. The data clearly show that LPS induces sialidase activity in live BMC-2 cells, and this activity is enhanced with increased cell numbers (Fig. 2d). The sialidase activity in each of the cell samples was calculated from a standard sialidase activity curve (Fig. 2e) and expressed as milli Units (mU) per mg of 4-MUNANA for each of the total cell number.

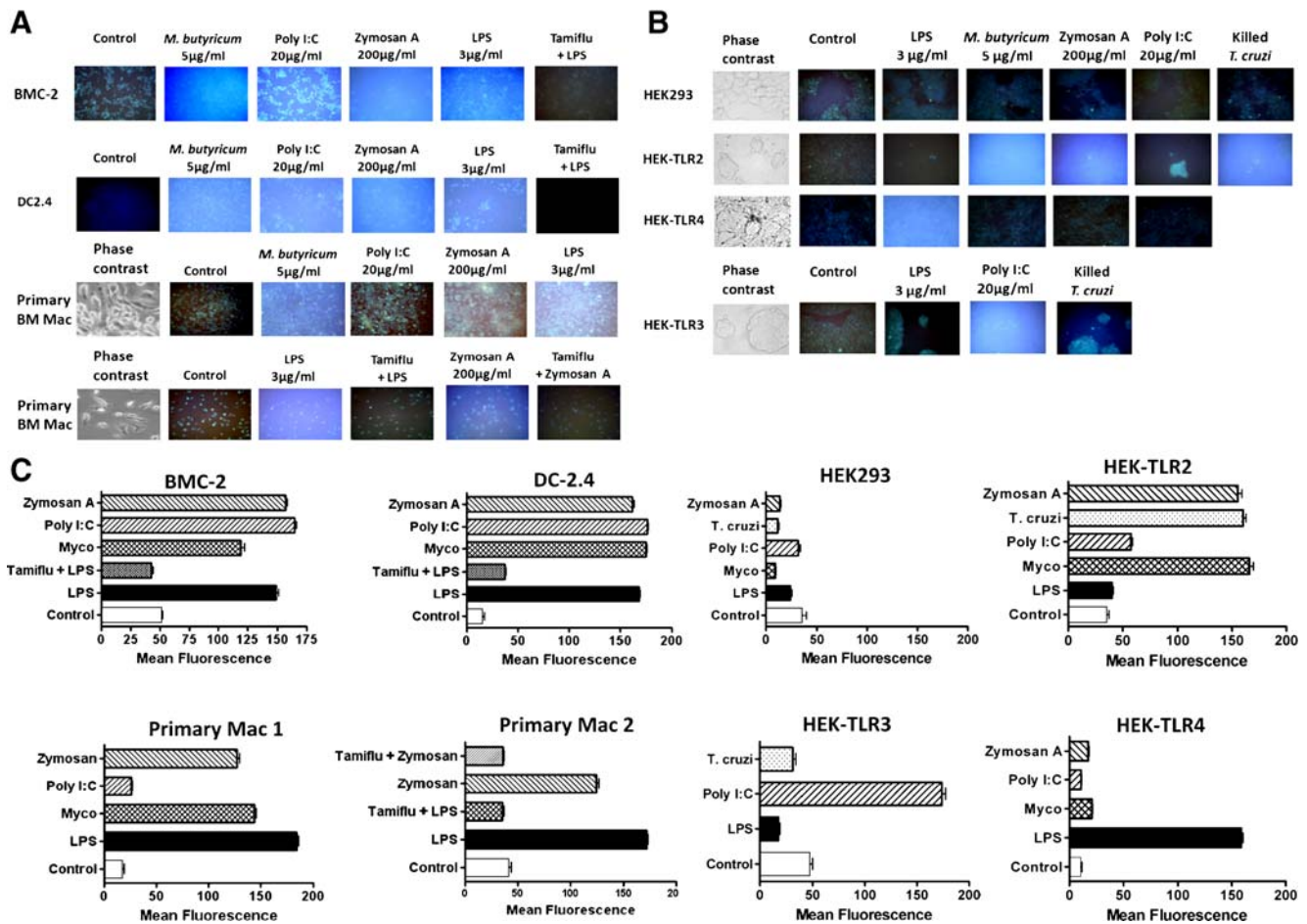


**Fig. 1 a** TLR ligands induce sialidase activity in live BMC-2 macrophage cells, DC2.4 dendritic cells and primary bone marrow macrophage (BM Mac) cells from normal, wild-type (WT) mice. BMC-2 and DC2.4 cells were allowed to adhere on 12 mm circular glass slides in media containing 5% horse and 3% fetal calf sera for 24 h. Primary BM macrophage cells were grown on 12 mm circular glass slides in RPMI conditioned medium for 7–8 days in a humidified incubator at 37°C and 5% CO<sub>2</sub>. After removing media, 0.318 mM 4-MUNANA (4-MU) substrate (2'-(4-methylumbelliferyl)- $\alpha$ -*N*-acetylneuraminic acid) in Tris buffered saline pH 7.4 was added to cells alone (Control), with TLR ligands (5  $\mu$ g/ml killed *Mycobacterium butyricum* cells, 20  $\mu$ g/ml purified Poly I:C, 200  $\mu$ g/ml purified Zymosan A, or 3  $\mu$ g/ml LPS phenol extracted from *Serratia marcescens*), or with ligand in combination with 200  $\mu$ M Tamiflu (oseltamivir phosphate). The substrate is hydrolyzed by sialidase enzymes to give free 4-methylumbelliferone, which has a fluorescence emission at 450 nm

(blue color) following excitation at 365 nm. Fluorescent images were taken at 2 min after adding substrate using epi-fluorescent microscopy (40x objective). The data are a representation of one out of three independent experiments showing similar results. **b** Sialidase activity is associated with TLR ligand treated live cells specific for TLR receptors. HEK293 or HEK-TLR2,-TLR3 and -TLR4/MD2 cells were allowed to adhere on 12mm circular glass slides and assayed as described in (a) above. Killed *T. cruzi* parasites (TLR2-agonist) were used in addition to the TLR ligands as in (a). After removing media, 0.318 mM 4-MU in Tris buffered saline pH 7.4 was added to cells alone (Control) or with the indicated TLR ligands. The data are a representation of one out of three independent experiments showing similar results. **c** The mean fluorescence surrounding the cells for  $n \geq 50$  replicates in each of the images was measured using MetaMorph 7 Software (Molecular Devices Corporation/MDS Analytical Technologies, Sunnyvale, CA)

#### Effect of neuraminidase inhibitors on TLR ligand induced sialidase activity in live macrophage cells

Next, we tested whether neuraminidase inhibitors would inhibit sialidase activity associated with TLR ligand treated live macrophage cells. Surprisingly, this TLR ligand induced sialidase activity was completely blocked by the neuraminidase inhibitor Tamiflu (pure oseltamivir phosphate) at 200  $\mu$ M as shown in Fig. 1a but also in a dose dependent range of 5–500  $\mu$ M (Fig. 3a). In addition,

other purified neuraminidase inhibitors such as BCX-1827 except BCX-1812, DANA (2-deoxy-2,3-dehydro-*N*-acetylneuraminic acid), zanamivir (4-guanidino-Neu5Ac2en), and oseltamivir carboxylate had a limited significant inhibition of LPS-induced sialidase activity in live BMC-2 cells at 1–2 mM compared to the LPS positive control (Fig. 3a). Other studies using recombinant soluble human sialidases have shown that oseltamivir carboxylate scarcely inhibited the activities of the four human sialidases even at 1 mM [17], while zanamivir significantly

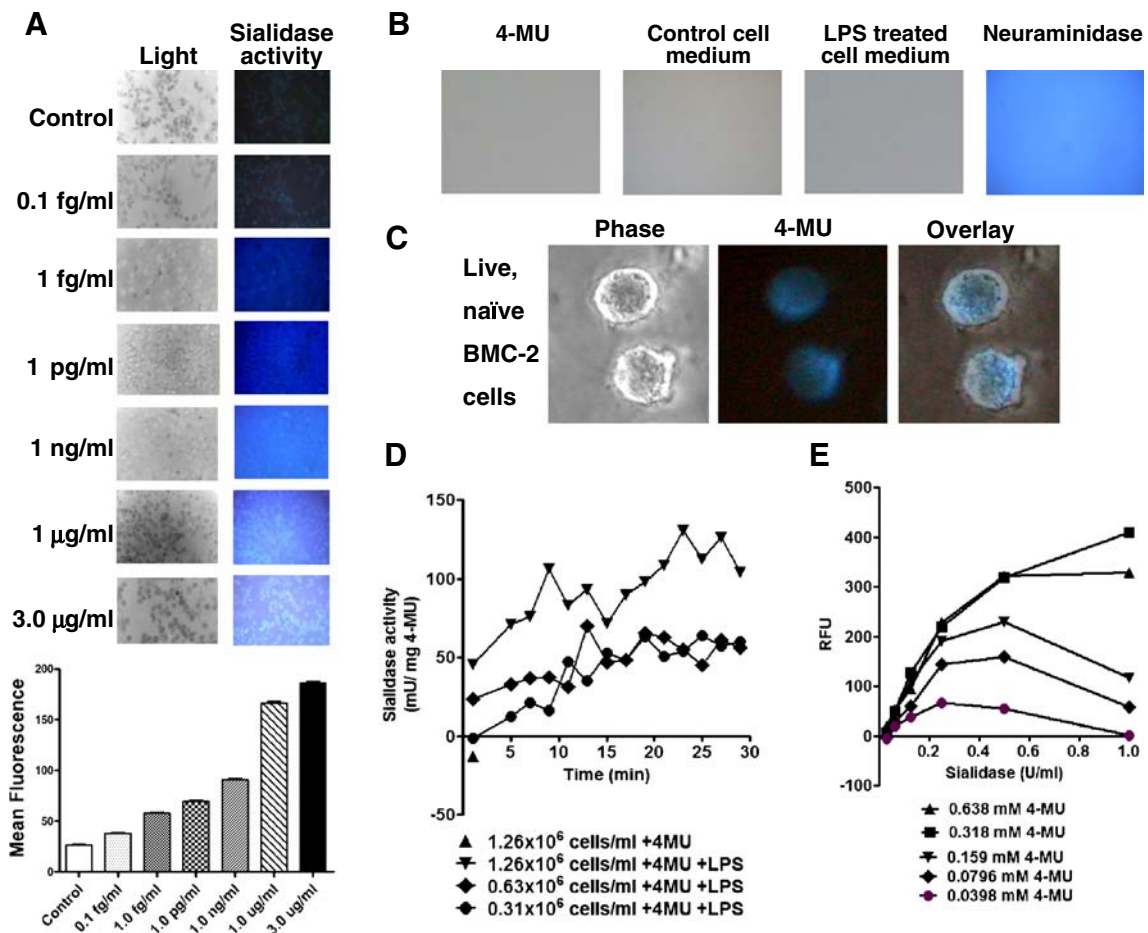


**Fig. 2** LPS induces sialidase activity in BMC-2 macrophage cells in a dose dependent manner. **a** LPS-induced sialidase activity in BMC-2 cells at the indicated doses was measured as described in Fig. 1a. Fluorescent images were taken at 1 min after adding substrate using epi-fluorescent microscopy (40x objective). The mean fluorescence surrounding the cells for each of the images was measured using MetaMorph 7 Software. The data are a representation of one out of three independent experiments showing similar results. **b** Medium (2 µL) was taken from control untreated live BMC-2 well or LPS (3 µg/mL; 5 min) treated well and added to 2 µL of 0.318 mM 4-MUNANA substrate. A positive control neuraminidase (*Clostridium perfringens*) (2 µL; with a specific activity of 1 U per 1.0 mmole of *N*-acetylneuraminic acid per minute) was added to 2 µL of 4-MUNANA substrate. Fluorescent images were taken at 1 min after adding substrate using epi-fluorescent microscopy (40x objective). **c** To live naïve BMC-2 cells was added 2 µL of 2.04 mM 4-MUNANA substrate. Fluorescent image was taken at 1 min after adding substrate using epi-fluorescent microscopy (40x objective). The image was enlarged to show cell fluorescence details. Adobe Photoshop was used to overlay the phase contrast image with the fluorescent cell image. **d** LPS-induced sialidase activity in cell suspensions of BMC-2 cells.

BMC-2 cells at 90% confluence in 25-cm<sup>2</sup> flasks were resuspended in 5 ml of Tris-buffered saline. 50 µL of 0.31 to 1.26 × 10<sup>6</sup> cells/mL was added to 5 µg/mL LPS and 0.318 mM 4-MU substrate and the remaining cells were left untreated as controls. The fluorescence intensity readings were immediately taken over 30 min using the Varioskan Fluorescence Spectrophotometer (Type 3001, Microplate Instrumentation, Thermo Electron Corporation, Vantaa, Finland) at emission 450 nm following an excitation at 365 nm. The sialidase activity in the cell samples was calculated from a standard sialidase activity curve, and expressed as milli Units per mg of 4-MUNANA after subtracting endogenous background sialidase activity in untreated cells. The mean ± SEM of the background endogenous sialidase activity in the control untreated live BMC-2 cells was 1.070 ± 0.43 mU per mg 4-MUNANA taken from four independent experiments. **e** Standard sialidase activity curve for optimum 4-MU substrate concentrations. 50 µL of neuraminidase (*Clostridium perfringens*; a specific activity of 1 U per 1.0 mmole of *N*-acetylneuraminic acid per minute) at different units/mL was added to 50 µL of 4-MU substrate at indicated concentrations. The relative fluorescence intensity readings (RFU) were immediately taken over 5 min using the Varioskan Fluorescence Spectrophotometer

inhibited the human Neu2 and Neu3 sialidases in the micromolar range. Furthermore, Nan *et al* using lysates from mature dendritic cells have found that zanamivir completely inhibited Neu1 and Neu3 sialidase activity at 2 mM [18].

It is interesting to note here that oseltamivir phosphate (Tamiflu) was found to be most potent compared to the other neuraminidase inhibitors in inhibiting the sialidase activity associated with TLR ligand treated live macrophage cells. Tamiflu is the ethyl ester pro-drug of the anti-

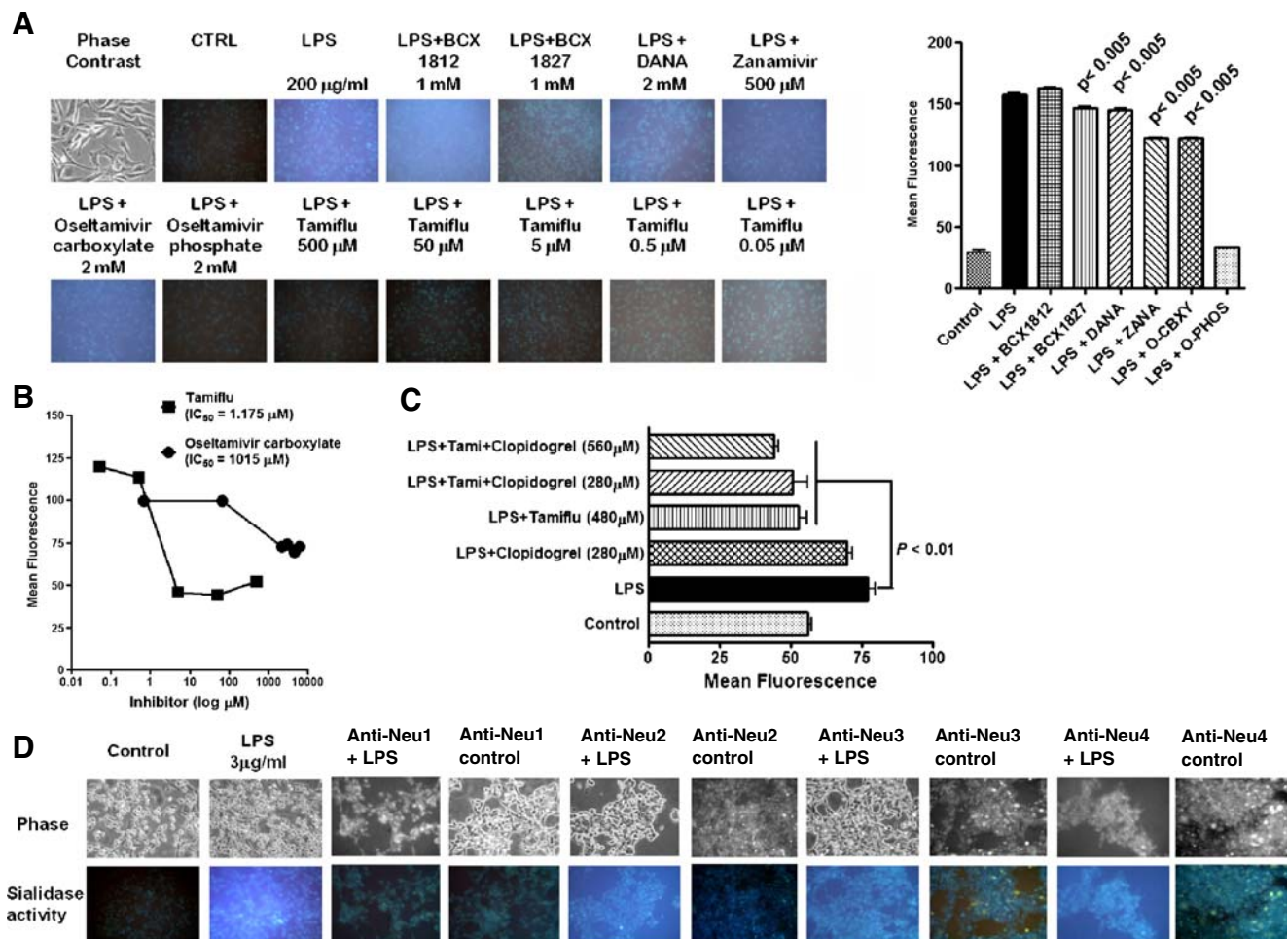


**Fig. 3** **a** Tamiflu completely inhibits LPS-induced sialidase activity in BMC-2 macrophage cells in a dose dependent manner while other indicated neuraminidase inhibitors have a limited inhibitory effect. LPS-induced sialidase activity in BMC-2 cells was measured as described in Fig. 1a. Fluorescent images were taken at 1 min after adding 0.318 mM 4-MU substrate together with LPS and indicated neuraminidase inhibitors (ZANA, zanamivir; O-CBXY, oseltamivir carboxylate; O-PHOS, oseltamivir phosphate) using epi-fluorescent microscopy (40x objective). The mean fluorescence surrounding the cells for each of the images was measured using MetaMorph 7 Software. The data are a representation of one out of three independent experiments showing similar results. Significant differences at 95% confidence using the Dunnett multiple comparison test was used to compare inhibition with the LPS control in each group for  $n=50$  replicates. **b** The 50% inhibition concentration (IC<sub>50</sub>) for Tamiflu and oseltamivir carboxylate on sialidase activity induced by LPS in live BMC-2 cells. Cells were treated with 5 µg/mL LPS in the presence or absence of different concentrations of the indicated inhibitors and 0.318 mM 4-MU substrate using epi-fluorescent

microscopy (40x objective) as described in Fig. 1a. The mean fluorescence surrounding the cells for each group was measured using MetaMorph 7 Software. The 50% inhibitory concentration (IC<sub>50</sub>) of each compound was determined by plotting the decrease in sialidase activity against the log of the agent concentration. **c** Anticarboxylesterase agent clopidogrel bisulfate on Tamiflu inhibition of sialidase activity induced by LPS in live BMC-2 cells. Cells were pretreated with clopidogrel bisulfate for 2 min followed by LPS in the presence or absence of Tamiflu as described in (b). Significant differences at 95% confidence using the Dunnett multiple comparison test was used to compare inhibition with the LPS control in each group for  $3 \leq n \leq 4$  independent experiments. **d** Inhibition of sialidase activity induced by LPS in live HEK-TLR4/MD2 cells by antibodies against human Neu1,-2,-3 and-4 sialidases. After removing media, 0.318 mM 4-MU substrate in Tris buffered saline pH7.4 was added to cells alone (Control), with 5 µg/ml LPS, antibody alone or with anti-Neu1 (12.5 µg/ml), anti-Neu2 (6.25 µg/ml), anti-Neu3 (62.5 µg/ml), or anti-Neu4 (21.8 µg/ml) neutralizing antibodies in combination with LPS using epi-fluorescent microscopy (40x objective) as described in Fig. 1a

influenza drug oseltamivir carboxylate, which is converted to this biologically active form *in vivo* [19]. Since Tamiflu is known to be ineffective *in vitro* because its antiviral activity is achieved by its hydrolytic metabolite oseltamivir carboxylate [20], we have actually observed the opposite effect in our live cell assay system. To further elucidate the

inhibitory capacity of Tamiflu and its hydrolytic metabolite oseltamivir carboxylate, the 50% inhibitory concentration (IC<sub>50</sub>) of each compound was determined by plotting the decrease in sialidase activity against the log of the agent concentration. As shown in Fig. 3b, Tamiflu had an IC<sub>50</sub> of 1.175 µM compared to an IC<sub>50</sub> of 1015 µM for oseltamivir



carboxylate. These data clearly illustrate that Tamiflu is 1000-fold more potent than its hydrolytic metabolite in inhibiting the sialidase activity associated with TLR ligand treated live BMC-2 macrophage cells. It is possible that Tamiflu could be transported through the cell membrane by a P-glycoprotein as recently described by Morimoto *et al* [21] where the hydrolytic activation could be catalyzed by carboxylesterase [20]. The antiplatelet agent clopidogrel has been previously determined to completely inhibit the hydrolysis of oseltamivir phosphate by carboxylesterase as much as 90% [20]. To determine whether or not this is the case in our live cell assay system, we pretreated live BMA macrophage cells with clopidogrel bisulfate at 280  $\mu$ M and 500  $\mu$ M for 2 min followed with 5  $\mu$ g/mL of LPS in the presence or absence of 400  $\mu$ M pure Tamiflu. The data in Fig. 3c indicate that the anticarboxylesterase agent clopidogrel had no effect on Tamiflu's capacity to inhibit LPS induced sialidase activity. Together, these results suggest that Tamiflu is a potent inhibitor of the sialidase associated with TLR ligand treated live macrophage cells.

Neu1 sialidase activity is associated with TLR ligand treated live macrophage cells

To identify the mammalian sialidase involved, we firstly used neutralizing antibodies against the four known human sialidases [22]. They are lysosomal Neu1 [18, 23–28], cytosolic Neu2 and the plasma membrane bound Neu3 [29–31]. The fourth sialidase Neu4 is localized to either the mitochondrial [32] compartment or the lysosomal lumen [33]. As shown in Fig. 3d, anti-Neu1 antibody blocked LPS-induced sialidase activity in live HEK-TLR4 cells compared with LPS positive control. In contrast, antibodies against Neu2, Neu3 or Neu4 had no blocking effect on LPS-induced sialidase activity in HEK-TLR4 cells. To confirm these results, we also used primary BM macrophages derived from the hypomorphic cathepsin A mice with the secondary ~90% reduction of the Neu1 activity (Neu1-CathA KD) [34]. After 7 days in culture with conditioned medium containing monocyte colony stimulating factor (M-CSF) [14], the primary macrophage cells were stimulated with TLR ligands to induce sialidase activity. The data indicated that all TLR ligands except TLR3 ligand polyI:C induce sialidase activity within 1 min in wild-type (WT), CathA KI (normal Neu1 sialidase bound to inactive cathepsin A Ser190Ala mutant) [34] and Neu4 KO (Neu4 knockout) [35] in primary BM macrophage cells derived from these mice (Fig. 4a). Furthermore, this sialidase activity associated with TLR ligand treated live primary macrophage cells from WT and Neu4 KO mice was blocked by Tamiflu or anti-Neu1 neutralizing antibody but not by anti-Neu3 antibody (Fig. 4a). Furthermore,

primary BM macrophage cells derived from Neu1-deficient mice (Neu1-CathA KD) exhibited no TLR ligand induced sialidase activity. These latter data provide evidence that Neu1 is involved in the TLR ligand induced sialidase activity.

To determine whether TLR ligand induced NF $\kappa$ B activation is dependent on Neu1 sialidase, we used primary BM macrophage cells derived from the Neu1-deficient mice. TLR4 ligand LPS and TLR2 ligand zymosan A induced NF $\kappa$ B activation localized to the nucleus in primary macrophage cells from WT (Fig. 4b) and CathA KI (Fig. 4c) mice, but not from the Neu1-deficient mice (Neu1-CathA KD) (Fig. 4d). When primary BM macrophages from Neu1 deficient mice were treated with purified *T. cruzi* trans-sialidase (TS) for 45 min in the absence of TLR ligand, the cells exhibited NF $\kappa$ B activation localized to the nucleus (Fig. 4d). Previously, we have shown that *T. cruzi* TS targets TrkA receptors and specifically hydrolyses sialyl  $\alpha$ 2-3-linked  $\beta$ -galactosyl residues [11]. When TLR deficient HEK293 cells were similarly treated with *T. cruzi* TS, they did not exhibit NF $\kappa$ B activation (data not shown). It is interesting to note here that exogenous  $\alpha$ 2,3-sialyl specific *T. cruzi* TS can override the Neu1-deficiency to activate NF $\kappa$ B in primary BM macrophage cells.

Neu1 sialidase colocalizes with TLR-2,-3 and-4 receptors on the cell surface in naïve macrophage cells

Since Neu1 sialidase is categorized as a lysosomal storage enzyme and it is induced within a minute on the cell surface membrane by TLR ligands, we asked how Neu1 can rapidly associate with TLR4 receptors on the cell surface. Using fluorescence microscopy, Neu1 was found on the cell surface in naïve, paraformaldehyde fixed and non-permeabilized BMC-2 macrophage cells (Fig. 5a). The immunolocalization of Neu1 to the cell surface was also confirmed by flow cytometry using live BMC-2 cells immunostained with anti-Neu1 antibody and Alexa488 conjugated secondary antibody. The data shown in Fig. 5b clearly indicate that 40000 acquired live cells showed significant immunostaining for Neu1 on the cell surface. Pshezhetsky *et al.* have also shown that during the differentiation of monocytes into macrophages, the majority of Neu1 relocates from the lysosomes to the cell surface, while the other cellular sialidases Neu2, Neu3 and Neu4, whose expression either remain unchanged or are down-regulated [24]. The lysosomal carboxypeptidase, cathepsin A, which forms a complex with and activates Neu1 in the lysosome, is also sorted to the plasma membrane of the differentiating cells. Hinek *et al.* have demonstrated that elastin-binding protein (EBP) forms a cell surface-targeted elastin receptor complex with cathepsin A and Neu1 sialidase, and provide evidence that this sialidase activity

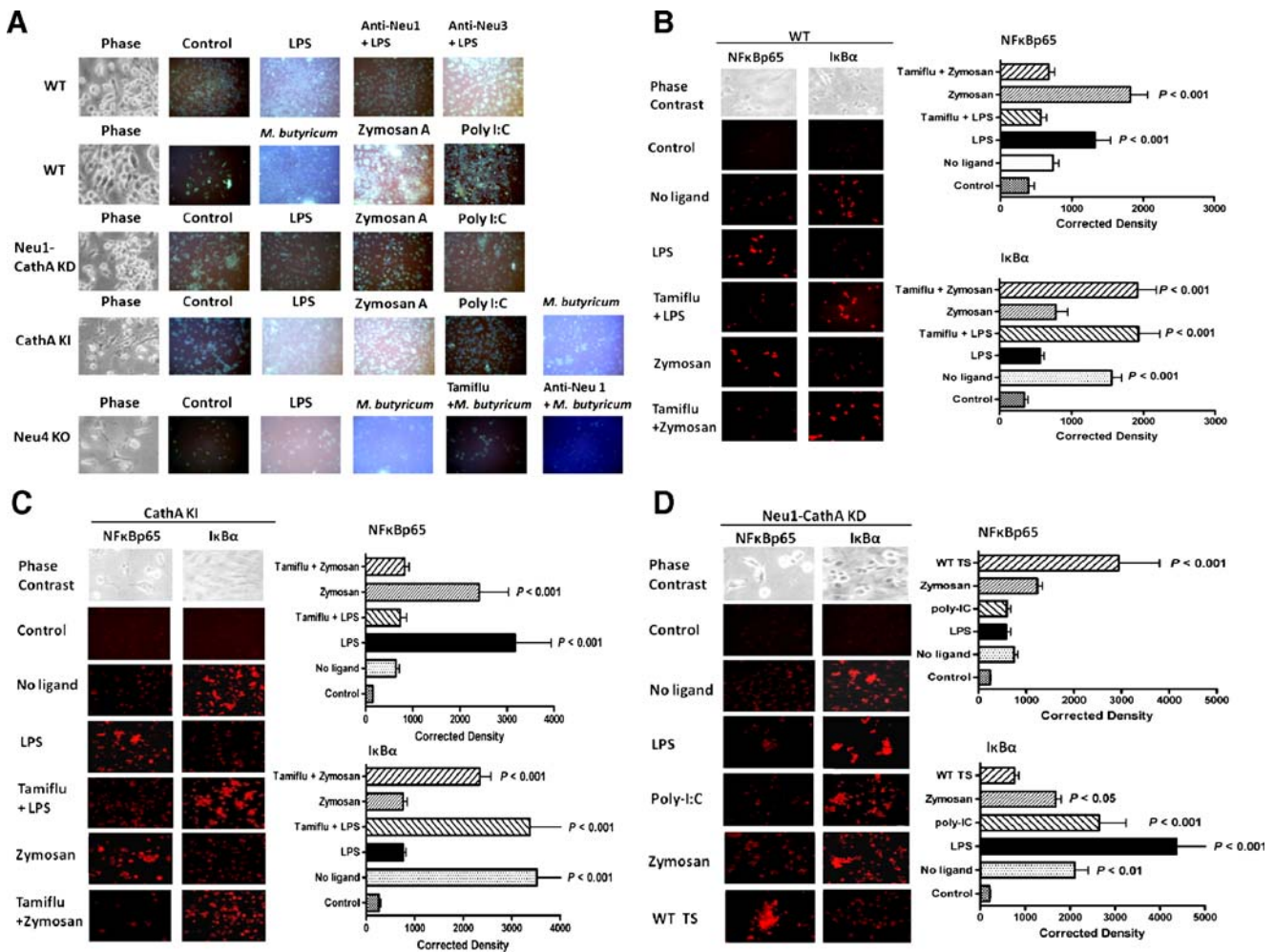


**Fig. 4** a TLR ligands induce sialidase activity in primary mouse BM macrophage cells. Primary BM macrophage cells obtained from normal, wild-type (WT), Neu1-CathA KD (Neu1 deficient and cathepsin A deficient), CathA KI (normal Neu1 bound to inactive cathepsin A), and Neu4 KO (Neu4 knockout) mice were cultured in conditioned medium supplemented with 20% (v/v) M-CSF, 10% FCS and Penn/Strep/Glut for 7–8 days on circular glass slides in 24 well tissue culture plates. After removing media, 0.318 mM 4-MU substrate was added to cells as in Fig. 1. For the WT and Neu4 KO groups, the indicated TLR ligands were added in combination with 12.5 μg/mL anti-Neu1 antibody, 62.5 μg/mL anti-Neu3 antibody or 200 μM Tamiflu. The data are a representation of one out of four independent experiments showing similar results. **b** Tamiflu blocks LPS- and Zymosan-induced NFκB activation in primary BM macrophage cells from normal, wild-type (WT) mice. Primary BM macrophage cells from WT mice were cultured as described in (a). Cells were pretreated with 200 μM Tamiflu for 30 min followed with either 3 μg/ml LPS or 200 μg/ml purified Zymosan A for 45 min. Cells were fixed with 4% paraformaldehyde, permeabilized with Triton-X100 and immunostained with rabbit anti-NFκBp65 or rabbit anti-IκBα followed with Alexa Fluor594 goat anti-rabbit IgG. Stained cells were visualized by epi-fluorescence microscopy using a 40x objective. Control images had no primary antibody. The no ligand images had only primary and secondary antibodies with no other treatment. Quantitative analysis was done by assessing the density of cell staining corrected for background in each panel using Corel Photo Paint 8.0 software. Each bar in the figures represents the mean

corrected density of culture cell staining ± SEM for equal cell density ( $5 \times 10^5$  cells) within the respective images. *P* values represent significant differences at 95% confidence using the Dunnett multiple comparison test compared to LPS treated cells. Approximately 90% of LPS-treated cells immunostained with anti-NFκBp65 antibody had nuclear staining. The data are a representation of one out of three independent experiments showing similar results. **c** Tamiflu blocks LPS- and Zymosan-induced NFκB activation in primary BM macrophage cells from CathA KI (normal Neu1 bound to inactive Cathepsin A) mice. Primary BM macrophages were cultured in RPMI conditioned medium as described in (a). Cells pretreated with 200 μM Tamiflu for 30 min followed with either 200 μg/ml purified Zymosan A or 3 μg/ml LPS for 45 min were paraformaldehyde fixed, permeabilized and immunostained for NFκBp65 and IκBα and quantitatively analyzed as described in (b). The data are a representation of one out of three independent experiments showing similar results. **d** Lack of LPS-, polyI:C- and Zymosan-induced NFκB activation in primary BM macrophage cells from Neu1-CathA KD (Neu1 deficient and Cathepsin A deficient) mice. Cells cultured in medium supplemented with 20% (v/v) M-CSF, 10% FCS and Penn/Strep/Glut for 7–8 days on circular glass slides in 24 well tissue culture plates were treated with 200 μg/ml purified Zymosan A, 3 μg/ml LPS for 45 min or 200 ng/ml TS for 60 min. Cells were paraformaldehyde fixed, permeabilized and immunostained for NFκBp65 and IκBα and quantitatively analyzed as described in (b). The data are a representation of one out of three independent experiments showing similar results

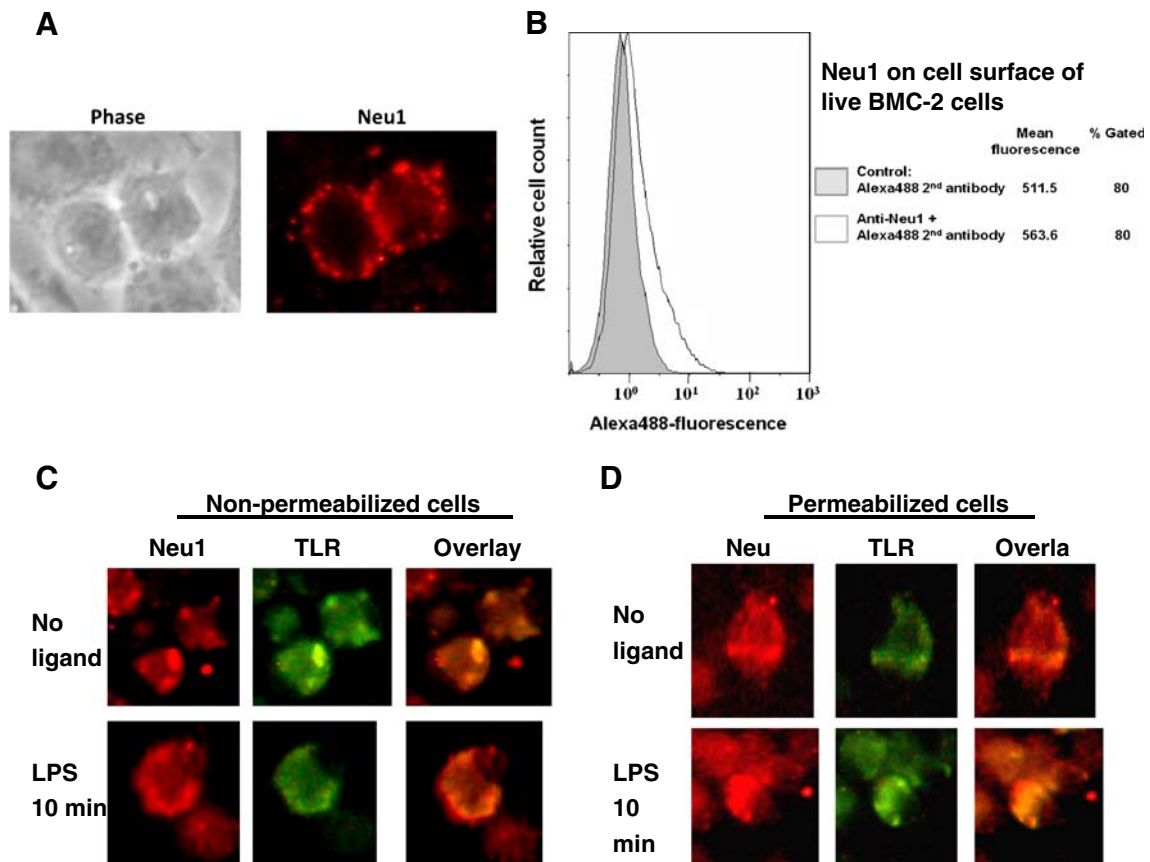


**Fig. 5 a** Neu1 on the cell membrane of BMC-2 cells. Untreated BMC-2 cells were fixed with 4% paraformaldehyde, non-permeabilized and immunostained with anti-Neu1 antibodies followed with Alexa594 conjugated secondary antibody. Stained cells were visualized using epi-fluorescence microscopy at objective 40x. The cell image panel was enlarged with Adobe Photoshop. **b** Flow cytometry analysis of Neu1 expressed on the cell surface of live BMC-2 cells. Histogram shows staining with rabbit anti-Neu1 antibodies after incubation on ice for 15 min and followed with Alexa488 conjugated secondary antibody for additional 15 min on ice. Control cells were stained with Alexa488 conjugated secondary antibody for 15 min on ice. Cells were analyzed by Beckman Coulter Epics XL-MCL flow cytometry and Expo32 ADC software (Beckman Coulter). Overlay histograms are displayed. Control Alexa488 secondary antibody treated cells are represented by the black-filled

histogram. Live cells stained with anti-Neu1 antibody are depicted by the unfilled histogram with the black line. The mean fluorescence for each histogram is indicated for 40000 acquired cells (80% gated). The data are a representation of one out of two experiments showing similar results. **c** and **d** Neu1 colocalizes with TLR4. Primary BM macrophage cells were stimulated with 5  $\mu$ g/mL LPS for 10 min or left untreated as control (no ligand). Cells were fixed with paraformaldehyde, non-permeabilized (**c**) or permeabilized (**d**) and immunostained with specific antibodies against Neu1 and TLR4 followed with respective Alexa Fluor conjugated secondary antibodies. Stained cells were visualized using a confocal inverted microscope (Leica TCS SP2 MP inverted Confocal Microscope) with a 100x objective (oil). The data are a representation of one out of three independent experiments showing similar results

is a prerequisite for the subsequent release of tropoelastin [26].

If Neu1 is localized to the cell surface, we asked whether or not it is associated with TLR receptors since sialidase activity is associated with TLR ligand treated live macrophage cells. Confocal microscopy revealed the cell-surface colocalization of Neu1 and TLR4 in naïve and LPS-treated non-permeabilized primary BM macrophage cells (Fig. 5c). Using confocal microscopy on permeabilized naïve and LPS-treated cells, the additional intracellular and cell-surface co-localization of Neu1 and TLR4 validated the predicted association of Neu1 with TLR receptors (Fig. 5d).

Co-immunoprecipitation experiments using HEK-TLR4/MD2 cells further demonstrated that Neu1 (Fig. 6a) and not Neu2,-3 or-4 (Fig. 6b) forms a complex with naïve or LPS-stimulated TLR4 receptors. Although Neu2,-3 and-4 were not detected in the lysates from co-immunoprecipitation with TLR4 receptor, they were present in the whole cell lysates from LPS-treated HEK-TLR4 cells (Fig. 6c). Since HEK-TLR4 cells have a specific chimeric TLR4 with an in frame C-terminal YFP, we were able to show that Neu1 also co-immunoprecipitated with TLR4 using anti-GFP antibodies (Fig. 6a). Conversely, TLR4 receptors co-immunoprecipitated with Neu1 in cell lysates from naïve

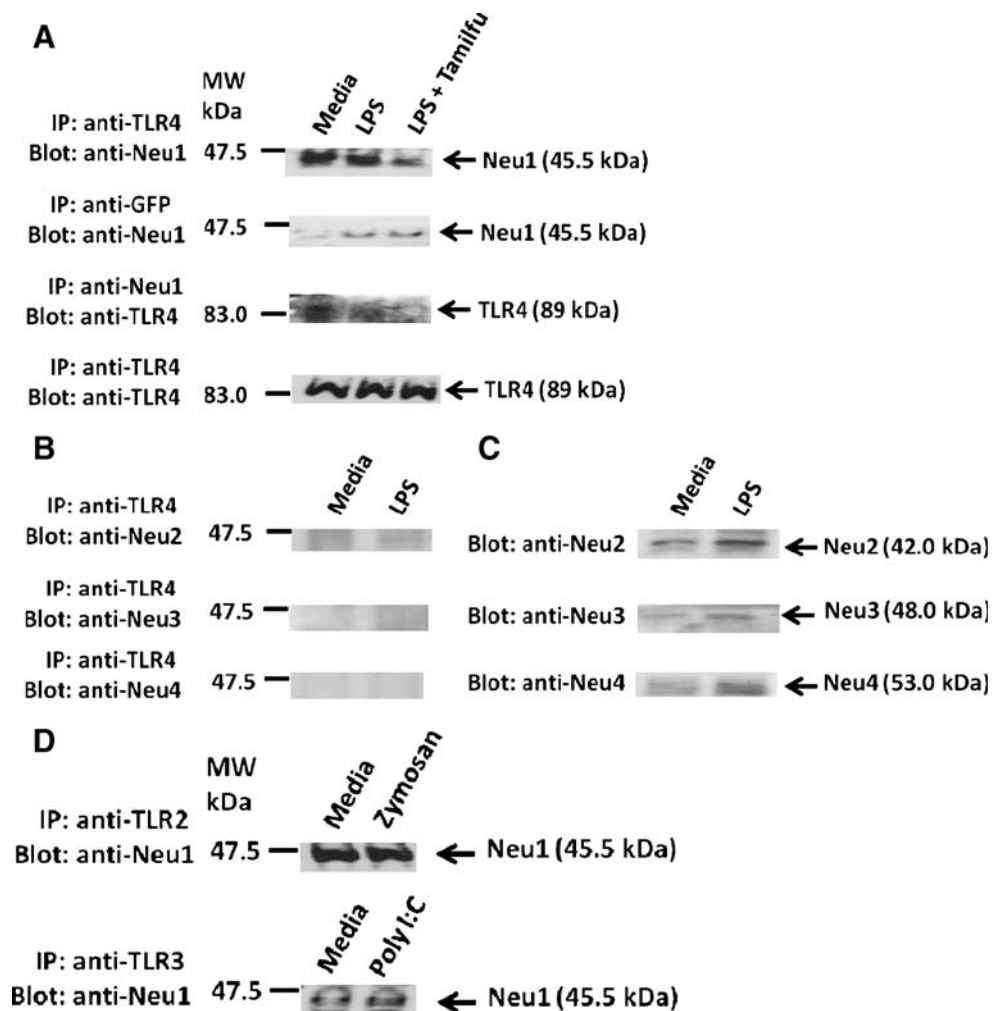


**Fig. 6** **a** Neu1 co-immunoprecipitates with TLR4. HEK-TLR4/MD2 cells with in-frame YFP were pretreated with 200  $\mu$ M Tamiflu for 30 min followed with 5  $\mu$ g/ml LPS for 5 min or left untreated as control (media). Cells were pelleted, lysed in lysis buffer and the protein lysates were immunoprecipitated with antibodies against the indicated proteins for 18 h. Immunocomplexes were isolated using protein G magnetic beads, resolved by SDS-PAGE and the blot probed with antibodies against the indicated proteins. The data are a representation of one out of five independent experiments showing similar results. **b** Neu2, 3 and 4 do not co-immunoprecipitate with

TLR4. HEK-TLR4/MD2 cells were used as described in (a). **c** Western blot analysis. HEK-TLR4/MD2 cells were pretreated with 5  $\mu$ g/ml LPS for 5 min or left untreated as control (media) as described in (a). They were pelleted, lysed in lysis buffer and the protein lysates were resolved by SDS-PAGE and the blot probed with antibodies against the indicated proteins. **d** Neu1 co-immunoprecipitates with TLR2 and -3. HEK-TLR2 and HEK-TLR3 cells were stimulated with 200  $\mu$ g/ml zymosan A or 20  $\mu$ g/ml polyIC, respectively or left untreated as media control. The cells were used as described in (a)

or LPS-treated HEK-TLR4 cells, but this was not seen in cell lysates from Tamiflu and LPS-treated cells. Perhaps, Tamiflu bound to Neu1 in cell lysates blocked anti-Neu1 antibodies in the immunoprecipitation assay. Surprisingly, Neu1 also co-immunoprecipitated with TLR2 and TLR3 receptors in naïve or ligand-treated HEK-TLR2 or HEK-TLR3 cells, respectively (Fig. 6d). Taken together, these results indicate that Neu1/TLR complexes are present on the cell membrane prior to ligand binding, which has not been previously observed. These findings suggest that Neu1 may be a common requisite intermediate in regulating pathogen-molecule induced TLR receptors.

Physiological relevance of Neu1 sialidase in regulating endotoxin LPS induced pro-inflammatory cytokines and nitric oxide production

If Neu1 sialidase activity is associated with TLR ligand treated live macrophage cells, we also asked if Neu1 has a physiological relevance in regulating endotoxin LPS induced pro-inflammatory cytokines and nitric oxide production. Using Neu1 deficient mice, we found that serum pro-inflammatory cytokines are induced in WT and Neu1-deficient mice responding to LPS after 5 h treatment when compared to basal serum levels (Fig. 7a).

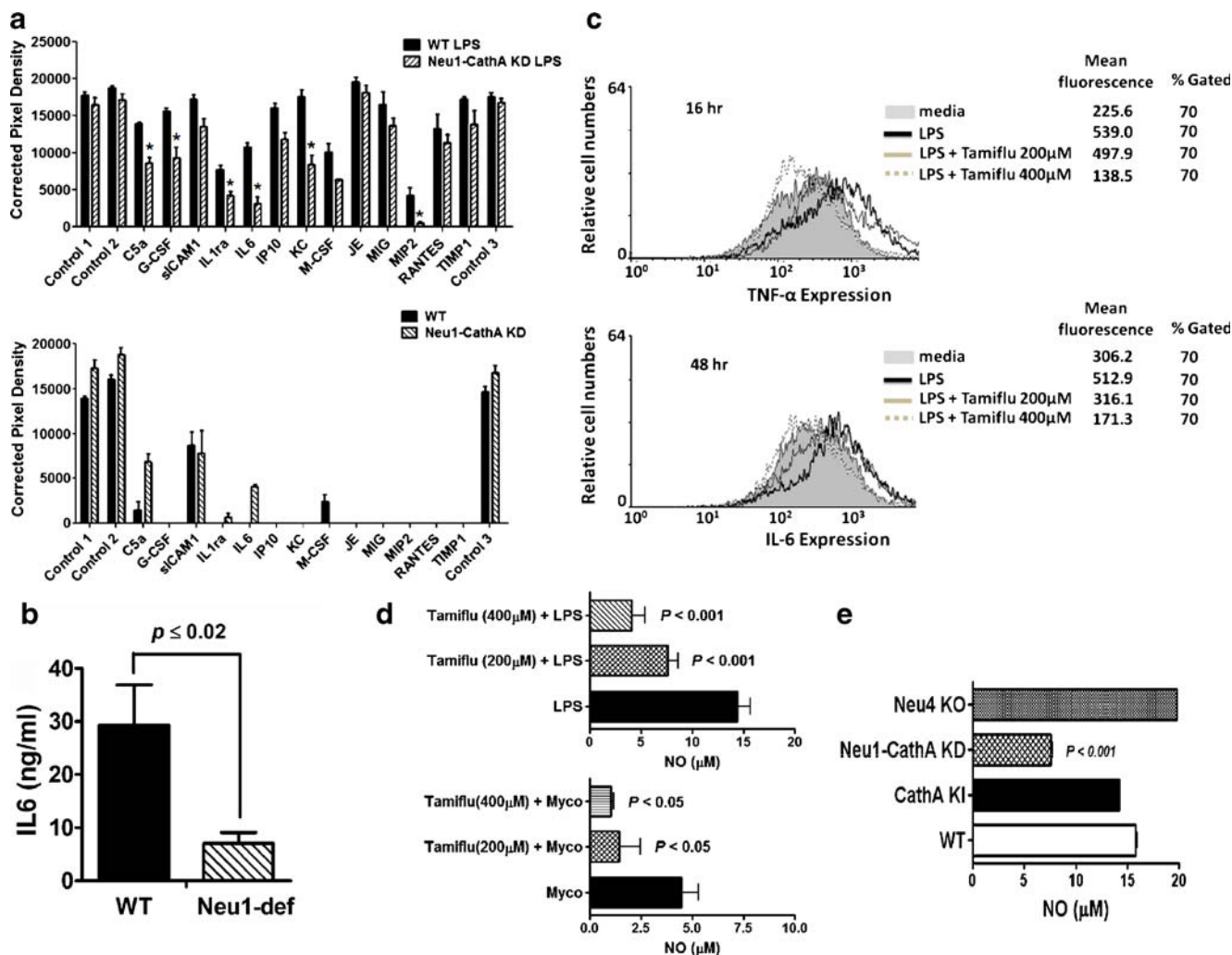


**Fig. 7 a** *In vivo* LPS induced serum cytokine production in normal, wild-type (WT) and Neu1-deficient mice. Four mice in each group were bled before (no LPS) and 5 h after i.p. injection with 2.5 mg of LPS per mouse. Serum was extracted from blood and immediately analyzed for cytokine array profiling with R&D System Cytokine Array Profiling kit. Quantitative analysis was done by assessing the density of spot staining corrected for background in each panel image using Corel Photo Paint 8.0 software. The histograms depict the pro-inflammatory cytokines. Asterisk (\*) represents significant differences at 95% confidence using the Dunnett multiple comparison test compared to WT group for  $n=4$  separate serum samples. **b** Serum from the same LPS treated mice was analyzed for IL-6 cytokine with eBioscience IL6 ELISA kit.  $P$  value represents significant differences at 95% confidence using the Dunnett multiple comparison test compared to WT group for  $n=4$  replicates. **c** Flow cytometry analysis of Tamiflu inhibition of LPS induced expression of TNF $\alpha$  (16 h) and IL-6 (48 h) in human monocytic THP-1 cells. Cells were pretreated with Tamiflu at indicated doses followed by 3  $\mu$ g/mL of LPS for 16 h (optimal time for TNF $\alpha$  expression) and for 48 h (optimal time for IL-6 expression) in the presence of Brefeldin A (BFA, Sigma). Cells were paraformaldehyde fixed, permeabilized and immunostained with fluorescein-conjugated anti-TNF $\alpha$  or anti-IL6 antibodies. Cells were analyzed by Beckman Coulter Epics XL-MCL flow cytometry and Expo32 ADC software (Beckman Coulter). Overlay histograms are displayed. Untreated control cells are represented by the gray-filled histogram. Cells pretreated with 200  $\mu$ M or 400  $\mu$ M of Tamiflu and stimulated with LPS are depicted by the gray-solid line or gray-dashed line, respectively. The mean fluorescence for each

histogram is indicated for 10,000 acquired cells (70% gated). The data are a representation of one out of three experiments showing similar results. **d** Nitrite (NO) production by dendritic cells stimulated with LPS or killed *M. butyricum* (Myco) is inhibited by Tamiflu. DC2.4 cells (50,000 cells/well) were pretreated with 200 or 400  $\mu$ M Tamiflu or left untreated in medium for 30 min followed with 1  $\mu$ g/ml LPS or 10  $\mu$ g/ml killed *M. butyricum* for 18 h. Supernatants were used to measure nitric oxide (NO) concentration after subtraction of control cells using the Griess reagent and standard concentration curve. The concentration of NO in the untreated control cells ranged from 5–7  $\mu$ M. The data are the mean  $\pm$  SEM of five independent experiments.  $P$  values represent significant differences at 95% confidence using the Dunnett multiple comparison test compared to LPS or Myco group for  $n=5$  independent experiments. **e** Nitrite (NO) production by primary BM macrophage cells derived from WT, Neu1-CathA KD, CathA KI and Neu4 KO mice stimulated with LPS. Primary BM macrophages obtained from normal, wild-type (WT), Neu1-CathA KD (Neu1 deficient and cathepsin A deficient), CathA KI (normal Neu1 bound to inactive cathepsin A) and Neu4 KO (Neu4 knockout) mice were cultured in conditioned medium as described in Fig. 4a. Primary cells (50,000 cells/well) were treated with 1  $\mu$ g/ml LPS or left untreated in medium for 18 h. Supernatants were used to measure nitric oxide (NO) concentration after subtraction of control cells using the Griess reagent and standard concentration curve as described in (d).  $P$  value represents significant differences at 95% confidence using the Dunnett multiple comparison test compared to LPS group for  $n=2$  independent experiments

However, the Neu1-deficient mice produced a significant diminution in C5a, G-CFS, IL1ra, IL-6, KC (cytokine-induced neutrophil chemoattractant) and MIP2 (macrophage inflammatory protein-2) cytokines in response to LPS compared to the WT mice. Using an IL-6 ELISA assay, serum IL-6 was significantly reduced in LPS treated Neu1 deficient mice compared to the WT (Fig. 7b).

We also determined whether Tamiflu treatment of human monocytic THP-1 in a dose dependent manner would inhibit IL-6 and TNF $\alpha$  production in response to LPS. Flow cytometric analyses (Fig. 7c) indicated this to be the case, suggesting that inhibition of the sialidase activity by the neuraminidase inhibitor Tamiflu is able to significantly inhibit LPS induced pro-inflammatory cytokine IL-6 and TNF $\alpha$  production in a dose dependent manner. In addition, Tamiflu significantly inhibited the production of nitric oxide (NO) in DC2.4 dendritic cells following LPS or killed *M. butyricum* (Myco) stimulation (Fig. 7d). These results are consistent with other reports indicating that oseltamivir reduces a synergy between influenza and IFN- $\gamma$  in NO synthesis within RAW 264.7 macrophages in a dose dependence manner [36]. To confirm Neu1 sialidase involvement in TLR4 ligand LPS induced NO production, we used primary BM macrophage cells from Neu1-deficient mice. As predicted, primary BM macrophage cells from Neu1-deficient mice exhibited a significant reduction in endotoxin LPS-induced NO production in comparison to WT (Fig. 7e). Primary BM macrophage cells derived CathA KI mice (normal Neu1 and inactive cathepsin A) or Neu4 knockout (KO) mice exhibited LPS-induced NO production comparable to the WT control (Fig. 7e). Taken together, TLR ligand induced pro-inflammatory IL-6 and TNF $\alpha$  cytokines and nitric oxide production are partially dependent on Neu1 sialidase.

## Conclusions

The molecular mechanisms by which TLR receptors become activated or even inhibited are not well understood. The data presented in this report provide evidence that Neu1 sialidase may be an important intermediate link in the initial process of ligand induced TLR activation and subsequent cell function. They indicate an initial rapid activation of Neu1 activity, which is only induced by TLR ligand binding. Central to this process is that Neu1 and not the other three mammalian sialidases forms a complex with TLR-2,-3 and-4 receptors in naïve macrophage cells. This would actually make Neu1 complexed with TLRs readily available to be induced upon TLR ligand binding. Our data support this premise, because the sialidase activity induced by TLR ligand treated live cells occurs within a minute. How Neu1 sialidase is rapidly induced by TLR ligand

binding to its receptor remains unknown. Perhaps, it can be speculated that TLR ligand binding to the ectodomain may lead to substantial conformational changes which might subsequently induce Neu1 sialidase activity. Indeed, others have demonstrated that binding of DNA containing CpG leads to substantial conformational changes in the TLR9 ectodomain [37–39].

Surprisingly, Tamiflu (oseltamivir phosphate), which is the ethyl ester pro-drug of oseltamivir carboxylate was found to be highly potent (IC<sub>50</sub> 1.175  $\mu$ M) in inhibiting Neu1 activity induced by TLR ligand treatment of live macrophage cells. The reason for this inhibitory potency of Tamiflu on Neu1 sialidase activity is unknown. However, it may be due to a unique orientation of Neu1 with the molecular multi-enzymatic complex that contains  $\beta$ -galactosidase and cathepsin A [23] and elastin-binding protein (EBP) [26], the complex of which would be associated within the ectodomain of TLR receptors. Stomatos *et al.* have also shown that Neu1 on the cell surface is tightly associated with a subunit of cathepsin A and the resulting complex influences cell surface sialic acid in activated cells and the production of IFN $\gamma$  [18]. It has also been shown using Neu1-deficient mice that they produce markedly less IgE and IgG1 antibodies following immunization with protein antigens, which may be the result of their failure to produce IL-4 cytokine [40]. In another study, Neu1 was found to negatively regulate lysosomal exocytosis in hematopoietic cells, where it processes the sialic acids on the lysosomal membrane protein LAMP-1 [25]. Taken all together, the potential significance of the role of Neu1 sialidase may be three-fold. Firstly, glycosylated TLR receptors have Neu1 bound together with cathepsin A and elastin binding protein at the ectodomain. Secondly, Neu1 may be a requisite intermediate in regulating TLR activation following TLR ligand binding to the receptor, and thirdly it may influence the receptor glycosylation in modulating TLR activation. The precise mechanism of how Neu1 influences receptor activation and cell function remains unknown.

In conclusion, the data presented in this report suggest that at least for TLR-2,-3 and-4 receptors the initial mechanism for TLR activation and subsequent cell function is dependent on Neu1 sialidase activity. Confocal microscopy and co-immunoprecipitation data indicate that Neu1/TLR complexes are already formed on the cell membrane in naïve primary macrophages or cell lines. Secondly, TLR ligand binding to its receptor may induce allosteric conformational changes in the TLR receptor, which in turn might activate Neu1 sialidase. It is proposed that activated Neu1 would then hydrolyze sialic acids to facilitate TLR dimerization and activation. It is known that LPS signals through TLR4 in complex with MD-2 and CD14, and each of these proteins is glycosylated [7, 41, 42]. MD-2 and the

amino terminal ectodomain of human TLR4 potentially contain two and nine *N*-glycosylation sites, respectively, based on their sequence analysis. Studies with TLR4 and MD-2 mutants lacking *N*-linked glycosylation sites have shown that these *N*-linked sites are essential to maintaining the functional integrity of this LPS receptor complex [7]. It is possible that potentially one or more of these *N*-linked glycosylation sites of TLR4/MD2 may be targets for Neu1 sialidase activity and thus they may play an important role in the activation of the TLR receptors and subsequent cellular bioactivity. The findings in this report suggest that Neu1 sialidase may be a key regulator of pathogen-molecule induced TLR activation to generate a functional receptor.

**Acknowledgements** These studies are partially supported by grants to MRS from Natural Sciences and Engineering Research Council of Canada (NSERC), the Harry Botterell Foundation for Neuroscience Research, ARC, and the Garfield Kelly Cardiovascular Research and Development Fund. S.R.A. is a recipient of the Queen's University Research Award, the Robert J. Wilson Fellowship and the Ontario Graduate Scholarship. P.J. is a recipient of the Queen's Graduate Award and the Robert J. Wilson Fellowship. SF is a recipient of the Ontario Graduate Scholarship in Science and Technology (OGSST). Work on KD mice is supported by grant to A.V.P. from Canadian Institutes of Health (CIHR). Research work on the TLR transfected cell lines is supported by grants to R.B. from the 'Interuniversitaire Attractiepoolen' (IAP6/18), the 'Fonds voor Wetenschappelijk Onderzoek-Vlaanderen' (FWO; grant 3G010505), and the 'Geconcerteerde Onderzoeksacties' of the Ghent University (GOA; grant 01G06B6).

**Author Contributions** M.R.S. and S.R.A. wrote the paper, designed and performed experiments; P.J. performed the WB and EMSA blots; S.F. did the neuraminidase inhibitor studies; S.S. performed the NO experiments; V.S. generated Neu1-deficient, Neu1-CathA, Neu4 KO mice; K.G., S.B., R.B. and A.V.P. helped with experiments and writing the paper; M.R.S. supervised the research design and the writing of the paper. All authors read and commented on the manuscript, and declare no competing financial interests.

## References

- Choe, J., Kelker, M.S., Wilson, I.A.: Crystal structure of human toll-like receptor 3 (TLR3) ectodomain. *Science* **309**, 581–585 (2005). doi:10.1126/science.1115253
- Bell, J.K., Botos, I., Hall, P.R., Askins, J., Shiloach, J., Segal, D.M., Davies, D.R.: The molecular structure of the Toll-like receptor 3 ligand-binding domain. *Proc. Natl. Acad. Sci. USA* **102**, 10976–10980 (2005). doi:10.1073/pnas.0505077102
- Miggin, S.M., O'Neill, L.A.: New insights into the regulation of TLR signaling. *J. Leukoc. Biol* **80**, 220–226 (2006). doi:10.1189/jlb.1105672
- Sun, J., Duffy, K.E., Ranjith-Kumar, C.T., Xiong, J., Lamb, R.J., Santos, J., Masarapu, H., Cunningham, M., Holzenburg, A., Sarisky, R.T., Mbow, M.L., Kao, C.: Structural and functional analyses of the human Toll-like receptor 3. Role of glycosylation. *J. Biol. Chem* **281**, 11144–11151 (2006). doi:10.1074/jbc.M510442200
- Leonard, J.N., Ghirlando, R., Askins, J., Bell, J.K., Margulies, D.H., Davies, D.R., Segal, D.M.: The TLR3 signaling complex forms by cooperative receptor dimerization. *Proc. Natl. Acad. Sci. USA* **105**, 258–263 (2008). doi:10.1073/pnas.0710779105
- Weber, A.N., Morse, M.A., Gay, N.J.: Four N-linked glycosylation sites in human toll-like receptor 2 cooperate to direct efficient biosynthesis and secretion. *J. Biol. Chem* **279**, 34589–34594 (2004). doi:10.1074/jbc.M403830200
- da Silva, C.J., Ulevitch, R.J.: MD-2 and TLR4 N-linked glycosylations are important for a functional lipopolysaccharide receptor. *J. Biol. Chem* **277**, 1845–1854 (2002). doi:10.1074/jbc.M109910200
- Watson, F.L., Porcionatto, M.A., Bhattacharyya, A., Stiles, C.D., Segal, R.A.: TrkA glycosylation regulates receptor localization and activity. *J. Neurobiol* **39**, 323–336 (1999). doi:10.1002/(SICI)1097-4695(199905)39:2<323::AID-NEU15>3.0.CO;2-4
- Woronowicz, A., Amith, S.R., De Vusser, K., Laroy, W., Contreras, R., Basta, S., Szewczuk, M.R.: Dependence of Neurotrophic Factor Activation of Trk Tyrosine Kinase Receptors on Cellular Sialidase. *Glycobiology* **17**, 10–24 (2007). doi:10.1093/glycob/cwl049
- Woronowicz, A., Amith, S.R., Davis, V.W., Jayanth, P., De Vusser, K., Laroy, W., Contreras, R., Meakin, S.O., Szewczuk, M.R.: Trypanosome trans-sialidase mediates neuroprotection against oxidative stress, serum/glucose deprivation, and hypoxia-induced neurite retraction in Trk-expressing PC12 cells. *Glycobiology* **17**, 725–734 (2007). doi:10.1093/glycob/cwm034
- Woronowicz, A., De Vusser, K., Laroy, W., Contreras, R., Meakin, S.O., Ross, G.M., Szewczuk, M.R.: Trypanosome trans-sialidase targets TrkA tyrosine kinase receptor and induces receptor internalization and activation. *Glycobiology* **14**, 987–998 (2004). doi:10.1093/glycob/cwh123
- Kovacsovic-Bankowski, M., Rock, K.L.: Presentation of exogenous antigens by macrophages: analysis of major histocompatibility complex class I and II presentation and regulation by cytokines. *Eur. J. Immunol* **24**, 2421–2428 (1994). doi:10.1002/eji.1830241024
- Shen, Z., Reznikoff, G., Dranoff, G., Rock, K.L.: Cloned dendritic cells can present exogenous antigens on both MHC class I and class II molecules. *J. Immunol* **158**, 2723–2730 (1997)
- Alatery, A., Basta, S.: An efficient culture method for generating large quantities of mature mouse splenic macrophages. *J. Immunol. Methods* **338**, 47–57 (2008). doi:10.1016/j.jim.2008.07.009
- Werling, D., Hope, J.C., Howard, C.J., Jungi, T.W.: Differential production of cytokines, reactive oxygen and nitrogen by bovine macrophages and dendritic cells stimulated with Toll-like receptor agonists. *Immunology* **111**, 41–52 (2004). doi:10.1111/j.1365-2567.2004.01781.x
- Lundberg, A.M., Drexler, S.K., Monaco, C., Williams, L.M., Sacre, S.M., Feldmann, M., Foxwell, B.M.: Key differences in TLR3/poly I:C signaling and cytokine induction by human primary cells: a phenomenon absent from murine cell systems. *Blood* **110**, 3245–3252 (2007). doi:10.1182/blood-2007-02-072934
- Hata, K., Koseki, K., Yamaguchi, K., Moriya, S., Suzuki, Y., Yingsakmongkon, S., Hirai, G., Sodeoka, M., von Itzstein, M., Miyagi, T.: Limited inhibitory effects of oseltamivir and zanamivir on human sialidases. *Antimicrob. Agents Chemother* **52**, 3484–3491 (2008). doi:10.1128/AAC.00344-08
- Nan, X., Carubelli, I., Stamatou, N.M.: Sialidase expression in activated human T lymphocytes influences production of IFN-gamma. *J. Leukoc. Biol* **81**, 284–296 (2007). doi:10.1189/jlb.1105692
- Mendel, D.B., Tai, C.Y., Escarpe, P.A., Li, W., Sidwell, R.W., Huffman, J.H., Sweet, C., Jakeman, K.J., Merson, J., Lacy, S.A., Lew, W., Williams, M.A., Zhang, L., Chen, M.S., Bischofberger, N., Kim, C.U.: Oral administration of a prodrug of the influenza virus neuraminidase inhibitor GS 4071 protects mice and ferrets

- against influenza infection. *Antimicrob. Agents Chemother* **42**, 640–646 (1998)
20. Shi, D., Yang, J., Yang, D., LeCluyse, E.L., Black, C., You, L., Akhlaghi, F., Yan, B.: Anti-influenza prodrug oseltamivir is activated by carboxylesterase human carboxylesterase 1, and the activation is inhibited by antiplatelet agent clopidogrel. *J. Pharmacol. Exp. Ther* **319**, 1477–1484 (2006). doi:10.1124/jpet.106.111807
  21. Morimoto, K., Nakakariya, M., Shirasaka, Y., Kakinuma, C., Fujita, T., Tamai, I., Ogihara, T.: Oseltamivir (Tamiflu) efflux transport at the blood-brain barrier via P-glycoprotein. *Drug Metab. Dispos* **36**, 6–9 (2008). doi:10.1124/dmd.107.017699
  22. Miyagi, T., Sagawa, J., Konno, K., Tsuiki, S.: Immunological discrimination of intralysosomal, cytosolic, and two membrane sialidases present in rat tissues. *J. Biochem* **107**, 794–798 (1990)
  23. Lukong, K.E., Elsliger, M.A., Chang, Y., Richard, C., Thomas, G., Carey, W., Tylki-Szymanska, A., Czartoryska, B., Buchholz, T., Criado, G.R., Palmeri, S., Pshezhetsky, A.V.: Characterization of the sialidase molecular defects in sialidosis patients suggests the structural organization of the lysosomal multienzyme complex. *Hum. Mol. Genet* **9**, 1075–1085 (2000). doi:10.1093/hmg/9.7.1075
  24. Feng, L., Seyrantepe, V., Landry, K., Ahmad, R., Ahmad, A., Stamos, N.M., Pshezhetsky, A.V.: Monocyte differentiation upregulates the expression of the lysosomal sialidase, neu1 and triggers its targeting to the plasma membrane via MHC class II-positive compartments. *J. Biol. Chem* **281**, 27526–27538 (2006). doi:10.1074/jbc.M605633200
  25. Yogalingam, G., Bonten, E.J., van de Vlekkert, D., Hu, H., Moshiah, S., Connell, S.A., d’Azzo, A.: Neuraminidase 1 is a negative regulator of lysosomal exocytosis. *Dev. Cell* **15**, 74–86 (2008). doi:10.1016/j.devcel.2008.05.005
  26. Hinek, A., Pshezhetsky, A.V., Von, I.M., Starcher, B.: Lysosomal sialidase (neuraminidase-1) is targeted to the cell surface in a multiprotein complex that facilitates elastic fiber assembly. *J. Biol. Chem* **281**, 3698–3710 (2006). doi:10.1074/jbc.M508736200
  27. Duca, L., Blanchevoye, C., Cantarelli, B., Ghoneim, C., Dedieu, S., Delacoux, F., Homebeck, W., Hinek, A., Martiny, L., Debelle, L.: The elastin receptor complex transduces signals through the catalytic activity of its Neu-1 subunit. *J. Biol. Chem* **282**, 12484–12491 (2007). doi:10.1074/jbc.M609505200
  28. Starcher, B., d’Azzo, A., Keller, P. W., Rao, G. K., Nadarajah, D., and Hinek, A.: Neuraminidase-1 is Required for the Normal Assembly of Elastic Fibers. *Am J Physiol Lung Cell Mol Physiol* (2008)
  29. Rodriguez, J.A., Piddini, E., Hasegawa, T., Miyagi, T., Dotti, C. G.: Plasma membrane ganglioside sialidase regulates axonal growth and regeneration in hippocampal neurons in culture. *J. Neurosci* **21**, 8387–8395 (2001)
  30. Sasaki, A., Hata, K., Suzuki, S., Sawada, M., Wada, T., Yamaguchi, K., Obinata, M., Tateno, H., Suzuki, H., Miyagi, T.: Overexpression of plasma membrane-associated sialidase attenuates insulin signaling in transgenic mice. *J. Biol. Chem* **278**, 27896–27902 (2003). doi:10.1074/jbc.M212200200
  31. Papini, N., Anastasia, L., Tringali, C., Croci, G., Bresciani, R., Yamaguchi, K., Miyagi, T., Preti, A., Prinetti, A., Prioni, S., Sonnino, S., Tettamanti, G., Venerando, B., Monti, E.: The plasma membrane-associated sialidase MmNEU3 modifies the ganglioside pattern of adjacent cells supporting its involvement in cell-to-cell interactions. *J. Biol. Chem* **279**, 16989–16995 (2004). doi:10.1074/jbc.M400881200
  32. Yamaguchi, K., Hata, K., Koseki, K., Shiozaki, K., Akita, H., Wada, T., Moriya, S., Miyagi, T.: Evidence for mitochondrial localization of a novel human sialidase (NEU4). *Biochem. J* **390**, 85–93 (2005). doi:10.1042/BJ20050017
  33. Seyrantepe, V., Poupetova, H., Froissart, R., Zobot, M.T., Maire, I., Pshezhetsky, A.V.: Molecular pathology of NEU1 gene in sialidosis. *Hum. Mutat* **22**, 343–352 (2003). doi:10.1002/humu.10268
  34. Seyrantepe, V., Hinek, A., Peng, J., Fedjaev, M., Ernest, S., Kadota, Y., Canuel, M., Itoh, K., Morales, C.R., Lavoie, J., Tremblay, J., Pshezhetsky, A.V.: Enzymatic activity of lysosomal carboxypeptidase (cathepsin) A is required for proper elastic fiber formation and inactivation of endothelin-1. *Circulation* **117**, 1973–1981 (2008). doi:10.1161/CIRCULATIONAHA.107.733212
  35. Seyrantepe, V., Canuel, M., Carpentier, S., Landry, K., Durand, S., Liang, F., Zeng, J., Caqueret, A., Gravel, R.A., Marchesini, S., Zwingmann, C., Michaud, J., Morales, C.R., Levade, T., Pshezhetsky, A.V.: Mice deficient in Neu4 sialidase exhibit abnormal ganglioside catabolism and lysosomal storage. *Hum. Mol. Genet* **17**, 1556–1568 (2008). doi:10.1093/hmg/ddn043
  36. Kacergius, T., Ambrozaitis, A., Deng, Y., Gravenstein, S.: Neuraminidase inhibitors reduce nitric oxide production in influenza virus-infected and gamma interferon-activated RAW 264.7 macrophages. *Pharmacol. Rep* **58**, 924–930 (2006)
  37. Latz, E., Verma, A., Visintin, A., Gong, M., Sirois, C.M., Klein, D.C., Monks, B.G., McKnight, C.J., Lamphier, M.S., Duprex, W. P., Espevik, T., Golenbock, D.T.: Ligand-induced conformational changes allosterically activate Toll-like receptor 9. *Nat. Immunol* **8**, 772–779 (2007). doi:10.1038/ni1479
  38. Haas, T., Metzger, J., Schmitz, F., Heit, A., Muller, T., Latz, E., Wagner, H.: The DNA sugar backbone 2' deoxyribose determines toll-like receptor 9 activation. *Immunity* **28**, 315–323 (2008). doi:10.1016/j.immuni.2008.01.013
  39. Ewald, S.E., Lee, B.L., Lau, L., Wickliffe, K.E., Shi, G.P., Chapman, H.A., Barton, G.M.: The ectodomain of Toll-like receptor 9 is cleaved to generate a functional receptor. *Nature* **456**, 658–662 (2008). doi:10.1038/nature07405
  40. Chen, X.P., Enioutina, E.Y., Daynes, R.A.: The control of IL-4 gene expression in activated murine T lymphocytes: a novel role for neu-1 sialidase. *J. Immunol* **158**, 3070–3080 (1997)
  41. Ohnishi, T., Muroi, M., Tanamoto, K.: N-linked glycosylations at Asn(26) and Asn(114) of human MD-2 are required for toll-like receptor 4-mediated activation of NF-kappaB by lipopolysaccharide. *J. Immunol* **167**, 3354–3359 (2001)
  42. Qiu, X.T., Li, Y.H., Li, H., Yu, Y., Zhang, Q.: Molecular cloning, mapping, and tissue expression of the porcine cluster of differentiation 14 (CD14) gene. *Biochem. Genet* **45**, 459–468 (2007). doi:10.1007/s10528-007-9088-8